Transient Kinetic Experiments Demonstrate the Existence of a Unique Catalytic Enzyme Form in the Peptide-Stimulated ATPase Mechanism of *Escherichia coli* Lon Protease†

Diana Vineyard, Xuemei Zhang, and Irene Lee*

Department of Chemistry, Case Western Reserve University, Cleveland, Ohio 44106

Received April 25, 2006; Revised Manuscript Received July 12, 2006

ABSTRACT: Lon is an oligomeric serine protease whose proteolytic activity is mediated by ATP hydrolysis. Although each monomeric subunit has an identical sequence, Lon contains two types of ATPase sites that hydrolyze ATP at drastically different rates. The catalytic low-affinity sites display pre-steady-state burst kinetics and hydrolyze ATP prior to peptide cleavage. The high-affinity sites are able to hydrolyze ATP at a very slow rate. By utilizing the differing K_d's, the high-affinity site can be blocked with unlabeled nucleotide while the activity at the low-affinity site is monitored. Little kinetic data are available that describe microscopic events along the reaction pathway of Lon. In this study we utilize MANT-ATP, a fluorescent analogue of ATP, to monitor the rate constants for binding of ATP as well as the release of ADP from *Escherichia coli* Lon protease. All of the adenine nucleotides tested bound to Lon on the order of 10^5 M^{-1} s^{-1}, and the previously proposed conformational change associated with nucleotide binding was also detected. On the basis of the data obtained in this study we propose that the rate of ADP release is slightly different for the two ATPase sites. As the model peptide substrate [S2; YRGITCSGRQK(Bz)] [Thomas-Wohlever, J., and Lee, I. (2002) *Biochemistry 41*, 9418−9425] or the protein substrate casein affects only the steady-state ATPase activity of the low-affinity sites, we propose that Lon adopts a different form after its first turnover as an ATP-dependent protease. Based on the obtained rate constants, a revised kinetic model is presented for ATPase activity in Lon protease in both the absence and presence of the model peptide substrate (S2).

Lon protease belongs to the AAA+ superfamily of ATPases because, like the other members (ClpXP, ClpAP, ClpCP, HslUV), its proteolytic activity is mediated by ATP hydrolysis (*1*−*10*). This family is based on multiple sequence alignments which define a common ATPase module and encompasses a broader range of proteins than the traditional AAA proteins (*A*TPases *a*ssociated with diverse cellular *a*ctivities) which are a subfamily of the Walker-type NTPases (*11*, *12*). Lon protease is distributed throughout the cytosol in prokaryotic cells while in eukaryotic cells it is localized to the mitochondria (*5*, *8*, *13*). Unlike the other members of the superfamily which consist of separate regulatory and proteolytic subunits, the lon gene encodes a single polypeptide subunit containing both the protease and ATPase domains (*12*). The subunits in Lon are organized into an oligomer shown in recently published partial crystal structures as a hexamer (*14*, *15*). The oligomerization of Lon results in a ring formation with a central cavity and is not dependent on ATP binding or hydrolysis (*16*, *17*).

Aside from the general interest surrounding Lon due to its unique coordination of ATPase activity with proteolytic function, Lon has been shown to be important in maintaining the virulence of various strains of pathogenic bacteria including *Salmonella enterica* serovar Typhimurium (*18*−*20*), *Brucella abortus* (*21*), and *Pseudomonas syringae* (*22*). However, the details surrounding the specific role of Lon in bacterial virulence are not clearly defined. A comprehensive understanding of the kinetic mechanism of Lon protease could prove useful in the future for targeting specific homologues with inhibitors. Because the protease and ATPase activity of Lon are inevitably intertwined, a clear understanding of the role of ATP hydrolysis activity in the enzyme is necessary.

The broadly defined in vivo function of Lon includes degrading misfolded or damaged proteins as well as short-lived regulatory proteins (*4*, *7*, *9*). Few physiological substrates of Lon have been identified because the substrate specificity is not well understood. One known substrate of the *Escherichia coli* Lon homologue is the λN protein (*7*, *23*). We have previously developed a small fluorescent peptide mimic of the λ N protein containing a single cleavage site (S3;[1] comprised of 10% fluorescent S1 peptide and 90% S2, the nonfluorescent analogue of S1) in order to easily monitor the kinetics of the *E. coli* Lon system (*24*, *25*). Although it is known that ATP mediates the protease activity in Lon, little definitive evidence exists for the timing of events and kinetic coordination of the two activities. Lon is known to bind to ADP with higher affinity than ATP, and the ATPase as well as peptidase activities of Lon are inhibited by ADP (*25*, *26*). Nonhydrolyzable analogues of ATP such as AMPPNP, which do not generate ADP, also

† This work was supported by NIH Grant GM067172.

* Corresponding author. Phone: 216-368-6001. E-mail: Irene.lee@case.edu. Fax: 216-368-3006.

10.1021/bi060809+ CCC: $33.50
Published on Web 08/23/2006

support Lon-mediated peptide cleavage with reduced catalytic efficiency (*24*). Although many observations have been made, it is not clear precisely how ADP release contributes to the catalytic mechanism of Lon. Using pre-steady-state kinetic methods, we have determined that there is a burst of ATP hydrolysis activity prior to the turnover of peptidase activity (*27*). The burst activity indicates that a step following ATP hydrolysis is rate limiting. This would be consistent with ADP release being rate limiting. The pre-steady-state ATPase activity was unusual because it displayed half-site reactivity, presumably due to the existence of two ATPase sites in Lon [$K_{d,high\ affinity} = 0.52\ \mu M$ (*26*, *27*), $K_{d,low\ affinity} = 10\ \mu M$ (*26*)]. The two ATPase sites are a result of monomeric subunits having different ATPase behavior in the oligomeric form of Lon, but they could not be distinguished structurally because only one identical sequence for an ATPase motif exists in each monomeric subunit. Therefore, kinetic studies to further investigate the differences in the activities of the high- and low-affinity ATPase sites in Lon protease were performed (*28*). The experiments presented in this referenced study capitalized on the differing affinities of the two sites. By manipulating the concentration of ATP present, the activity of the high- and low-affinity sites could be monitored separately. The results showed that at stoichiometric concentrations of Lon and ATP (6 μM Lon, 6 μM ATP) the high-affinity sites were slowly processing ATP at 0.01 s^{-1}. Although a previously published pulse−chase experiment already confirmed that only one set of sites was responsible for the pre-steady-state burst (*27*), we examined the low-affinity ATPase sites by blocking the high-affinity ATPase sites with stoichiometric amounts of unlabeled nucleotide. The low-affinity sites hydrolyzed ATP faster (17 s^{-1}) than the high-affinity sites and were found to be solely responsible for the pre-steady-state burst in ATPase activity. The activity of each site apparently had no effect on the other's activity. Typically, a 2−5-fold stimulation of steady-state ATPase activity is observed in the presence of peptide or protein substrate (*5*, *25*, *29*). Interestingly, this stimulation was lost if the high-affinity ATPase sites were blocked with stoichiometric amounts of ATP, suggesting that the peptide substrate stimulates steady-state ATP hydrolysis at the high-affinity sites. However, given the information gleaned from the present study, the high-affinity sites seem to essentially be noncatalytic. So the reduced steady-state activity noted in the past study was more likely a result of ADP product inhibition of the low-affinity sites, rather than the peptide not being able to stimulate activity of the low-affinity ATPase sites.

These previous pre-steady-state kinetic studies of *E. coli* Lon protease have only addressed the hydrolysis portions of the ATPase mechanism at the high- and low-affinity sites (*27*, *28*). In the present study the rate of ATP binding and ADP release from the two ATPase sites was investigated in order to achieve a better understanding of the overall kinetic mechanism. We used the fluorescent 2′- (or 3′-) *O*-(*N*-methylanthraniloyl) (MANT) nucleotide analogues to accomplish this goal. In order to use this analogue, MANT-ATP was first shown to support S3 peptide hydrolysis, induce a conformational change, and be hydrolyzed by *E. coli* Lon protease comparably to ATP. The on rate of binding to the high- and low-affinity ATPase sites was measured and found to be on the order of $10^5\ M^{-1}\ s^{-1}$. A conformational change upon nucleotide binding was also detected, confirming previous hypotheses (*30*). The off rate of ADP, however, differed slightly for each of the ATPase sites, and although this step was proposed to be rate limiting in steady-state studies, ADP release only limited the low-affinity ATPase turnover. Because S2 peptide affected none of the pre-steady-state rate constants, we propose a novel enzyme form that exists after the first round of cleavage which undergoes catalytic ATPase turnover in the presence of peptide. We therefore revise our current kinetic model to accommodate the newly obtained results.

MATERIALS AND METHODS

Materials. Nucleotides were purchased from Sigma or ICN Biomedical. PNPase and 7-MEG were purchased from Sigma. Fmoc-protected amino acids, Boc-Abz, Fmoc-protected Lys Wang resin, and HBTU were purchased from Advanced ChemTech and Nova Biochem. Tris, HEPES, SBTI, and TPCK-treated trypsin were purchased from Fisher. MANT-AMPPNP and MDCC were purchased from Molecular Probes. Cloning reagents were purchased from Promega, New England BioLabs Inc., Invitrogen, and USB Corporations. Oligonucleotides were purchased from Integrated DNA Technologies Inc.

General Methods. Peptide synthesis and protein purification procedures were performed as described previously (*24*). Synthesis of MANT-ATP and MANT-ADP was performed as described previously (*31*, *32*). All enzyme concentrations were reported as Lon monomer concentrations. All reagents are reported as final concentrations. Unless otherwise stated all experiments were performed at 37 °C.

Cloning and Purification of Phosphate Binding Protein (PBP). The phosphate binding protein (PBP) gene with the attached phoS signal sequence was amplified from genomic DNA of the DH5α strain of *E. coli* using the forward primer 5-GGAATTCCATATGAAAGTTATGCGTACC-3′ and the reverse primer 5′-CCCAAGCTTTTATTAGTACAGCGG-3′. An A197C mutation was then introduced using PCR primer site-directed mutagenesis and the additional forward primer 5′-GTTGAATATTGTTACGCGAAG-3′ and reverse primer 5′-CCTCGCGTAACAATATTCAAC-3′. The resulting product was cloned into the *Hin*dIII and *Nde*I sites of the pET-24c(+) vector and the resulting plasmid named pHF019. This subcloned phosphate binding protein from *E. coli* DH5α contained one residue (Y306F) which differed

[1] Abbreviations: AMPPNP, adenylyl 5-imidodiphosphate; DTT, dithiothreitol; Abz, anthranilamide; Bz, benzoic acid amide; HBTU, *O*-benzotriazole *N*,*N*,*N*′,*N*′-tetramethyluronium hexafluorophosphate; HEPES, *N*-(2-hydroxyethyl)piperazine-*N*′-2-ethanesulfonic acid; Tris, 2-amino-2-(hydroxymethyl)-1,3-propanediol; KP_i, potassium phosphate; $Mg(OAc)_2$, magnesium acetate; KOAc, potassium acetate; SBTI, soybean trypsin inhibitor; PEI−cellulose, polyethylenimine−cellulose; PBP, phosphate binding protein; MDCC, 7-diethylamino-3-[[[(2-maleimidyl)ethyl]amino]carbonyl]coumarin; MDCC-PBP, A197C mutant of PBP labeled with MDCC; MANT, 2′- (or 3′-) *O*-(*N*-methylanthraniloyl); PNPase, purine nucleoside phosphorylase; MEG, 7-methylguanosine; P_i, inorganic phosphate; S2, a nonfluorescent analogue of S3 that is degraded by Lon identically as S3 and is used in the ATPase reactions to conserve the fluorescent peptide (S3) YRGITCSGRQK(Bz); S3, a mixed peptide substrate containing 10% of the fluorescent peptide $Y(NO_2)$RGITCSGRQK(Abz) and 90% S2; NTP, nucleotide triphosphate; SSD, the substrate sensor and discriminatory domain in Lon which is thought to interact with peptide substrate, resulting in allosteric behavior.

from the originally cloned protein. pHF019 was overexpressed in BL21(DE3), selected for with 30 μg/mL kanamycin, and induced at $OD_{600} = 1.5$ with 1 mM IPTG. The protein was isolated by osmotic lysis and purified to homogeneity as reported previously by Martin R. Webb and colleagues (National Institute of Medical Research, Mill Hill, London). This purification procedure and labeling of C197 with MDCC are described in detail in ref *33*. The purified labeled protein exhibits activity (excitation 425 nm, emission 465 nm) that is comparable to that observed in the PBP purified from the original cell strain (a generous gift from Susan Gilbert, University of Pittsburgh) developed by Webb and colleagues.

Steady-State MANT-ATPase Assays Using MDCC-PBP. Steady-state velocity data for MANT-ATP and ATP were measured using an assay to detect inorganic phosphate (P_i) release as described previously (*33*, *34*). Reactions contained 50 mM Tris at pH 8.0, 5 mM $Mg(OAc)_2$, 2 mM DTT, 150 μM 7-methylguanosine (MEG), 0.05 unit/mL PNPase, 300 or 150 nM *E. coli* Lon, ±500 μM S2 peptide, and 25 μM−1 mM MANT-ATP or ATP. ATPase activity was monitored on a Fluoromax 3 spectrofluorometer (Horiba Group) where fluorescent MDCC-PBP was excited at 425 nm and emitted at 465 nm. The velocity reactions were equilibrated at 37 °C for 1 min and initiated with the addition of Lon. Initial velocities were determined from plots of the amount of P_i released versus time. All assays were performed at least in triplicate, and the kinetic parameters were determined by fitting the averaged rate constant data with eq 1 using the nonlinear regression program KaleidaGraph (Synergy) version 3.6:

$$k_{obs} = k_{cat}[ATP]/(K_m + [ATP]) \quad (1)$$

where k_{obs} is the observed rate constant in s^{-1}, k_{cat} is the maximal rate in s^{-1}, [ATP] is the nucleotide concentration in μM, and K_m is the Michaelis−Menten constant in μM.

Peptidase Methods. Peptidase activity was monitored on a Fluoromax 3 spectrofluorometer (Horiba Group) as described previously (*25*). Assays contained 50 mM HEPES, pH 8.0, 75 mM KOAc, 5 mM DTT, 5 mM $Mg(OAc)_2$, 200 nM *E. coli* Lon, 150 μM MANT-ATP or ATP, 50−150 μM S1 peptide (100% fluorescent), and 200 μM−1.5 mM S3 peptide (10% fluorescent S1 peptide, 90% nonfluorescent analogue S2 peptide) (excitation 320 nm, emission 420 nm). Initial velocities were determined from plots of relative fluorescence versus time. All assays were performed at least in triplicate, and the kinetic parameters were determined by fitting the averaged rate constant data with eq 2 using the nonlinear regression program KaleidaGraph (Synergy) version 3.6:

$$k = k_{max}[S]^n/(K' + [S]^n) \quad (2)$$

where k is the observed rate constant being measured in units of seconds, k_{max} is the maximum rate constant referred to as $k_{ss,S3}$ in units of s^{-1}, [S] is the variable peptide substrate in units of μM, K' is the Michaelis constant for [S], and n is the Hill coefficient. The K_s (μM) is calculated from the relationship $\log K' = n \log K_s$, where K_s is the [S] required to obtain 50% of the maximal rate constant of the reaction referred to as $K_{m,ATP}$ or $K_{m,MANT-ATP}$.

Tryptic Digestions. Tryptic digest reactions were monitored as described previously (*28*, *30*). Briefly, 1.4 μM Lon in a reaction mixture containing 50 mM HEPES (pH 8.0), 5 mM $Mg(OAc)_2$, 2 mM DTT, ±800 μM S2 peptide, and 1 mM ATP, 1 mM MANT-ATP, 1 mM ADP, 1 mM MANT-ADP, 1 mM AMPPNP, or 1 mM MANT-AMPPNP was started by the addition of 1/50 (w/w) TPCK- (*N*-*p*-tosyl-L-phenylalanine chloromethyl ketone) treated trypsin with respect to Lon. At 0 and 30 min, a 3 μL reaction aliquot was quenched in 3 μg of soybean trypsin inhibitor (SBTI) followed by boiling. The quenched reactions were resolved by 12.5% SDS−PAGE analysis and visualized with Coomassie brilliant blue.

MANT-ATP Binding Time Courses by Fluorescent Stopped Flow. Pre-steady-state experiments were performed on a KinTek Stopped Flow controlled by the data collection software Stop Flow version 7.50 β. The sample syringes were maintained at 37 °C by a circulating water bath. Syringe A contained 5 μM *E. coli* Lon monomer with and without 500 μM S2 peptide, 5 mM $Mg(OAc)_2$, 50 mM HEPES, pH 8, 75 mM KOAc, and 5 mM DTT. Syringe B contained varying amounts of MANT-ATP, MANT-dATP, MANT-ADP, or MANT-AMPPNP (1−100 μM), 5 mM $Mg(OAc)_2$, 50 mM HEPES, pH 8, 75 mM KOAc, and 5 mM DTT. MANT−nucleotide binding was detected by an increase in fluorescence (excitation 360 nm, emission 450 nm) resulting from rapid mixing of the syringe contents in the sample cell. The resulting exponential data were a result of averaging at least four traces. All experiments were performed at least in triplicate. The averaged time courses were fit with the equation:

$$Y = (A_1 \exp^{-k_1 t} + C1) + (A_2 \exp^{-k_2 t} + C2) \quad (3)$$

where t is time in seconds, A_1 and A_2 are amplitudes for the first and second exponential phases, respectively, in relative fluorescence units, k_1 and k_2 are the observed rate constants for the first and second exponential phases in seconds, and C1 and C2 are constants.

MANT-ADP Release Time Courses by Fluorescent Stopped Flow. Pre-steady-state experiments were performed on a KinTek Stopped Flow controlled by the data collection software Stop Flow version 7.50 β. The sample syringes were maintained at 37 °C by a circulating water bath. Syringe A contained 5 μM *E. coli* Lon monomer with and without 500 μM S2 peptide which was preincubated with varying amounts of MANT-ADP (10 min), MANT-ATP, and MANT-dATP (30 min, 37 °C) (0.05−200 M), in 5 mM $Mg(OAc)_2$, 50 mM HEPES, pH 8, 75 mM KOAc, and 5 mM DTT. Syringe B contained 1 mM ADP, 5 mM $Mg(OAc)_2$, 50 mM HEPES pH 8, 75 mM KOAc, and 5 mM DTT. MANT-ADP release was detected by a decrease in fluorescence (excitation 360 nm, emission 450 nm) resulting from rapid mixing of syringe contents in the sample cell. The resulting exponential data were a result of averaging at least four traces. All experiments were performed in triplicate and the averaged time courses fit with eq 3.

Double mixing experiments were performed as above with the following exceptions. The valve for syringe C was opened on the KinTek Stopped Flow and the delay line calibrated at 33 μL, resulting in a second push volume of 46 μL. Syringe A contained 5 mM *E. coli* Lon monomer and 5 mM

ADP in 5 mM $Mg(OAc)_2$, 50 mM HEPES, pH 8, 75 mM KOAc, and 5 mM DTT. Syringe B contained 1 mM ADP with or without 500 μM S2 in 5 mM $Mg(OAc)_2$, 50 mM HEPES, pH 8, 75 mM KOAc, and 5 mM DTT. Syringe C contained 100 μM MANT-ADP or ATP in 5 mM $Mg(OAc)_2$, 50 mM HEPES, pH 8, 75 mM KOAc, and 5 mM DTT. The contents of syringes A and C were rapidly mixed with a first reaction time of 50 s for MANT-ATP and 3 ms for MANT-ADP. The second push would then mix the developed reaction from syringes A and C with the contents of syringe B in the observation cell in order to monitor the release of MANT-ADP from Lon over 30 s. All experiments were performed at least in triplicate and the averaged time courses fit with a single exponential equation.

RESULTS

Steady-State Characterization of the MANT-ATPase Activity of Lon. In order to perform pre-steady-state stopped-flow experiments to determine the rate constants associated with ATP binding and ADP release, a fluorescent analogue of ATP was needed. To determine if the *N*-methylanthraniloyl (MANT) fluorescently labeled ATP was also a substrate of Lon protease, and thus an appropriate analogue of unlabeled ATP, the steady-state kinetics of MANT-ATP hydrolysis were examined in comparison to ATP hydrolysis. This was accomplished using a coupled assay system with MDCC-PBP on a Fluoromax 3 spectrofluorometer (Horiba Group) as described previously (*33*, *34*). Phosphate binding protein (PBP) is the product of the *phoS* gene in *E. coli* which is induced when the levels of P_i are low, is localized to the periplasmic space, and is implicated in the transport of P_i (*33*, *35*). Martin Webb and colleagues (National Institute for Medical Research) introduced the mutation A197C in PBP in order to covalently label the introduced cysteine with a fluorophore (*33*). By doing this, they created a probe for P_i which can rapidly measure micromolar concentrations released from enzymes in real time due to the increase in fluorescence resulting from MDCC-PBP binding P_i. In order to reduce the extraneous P_i contamination, the cuvettes were soaked in a phosphate "mop" solution consisting of 150 μM MEG and 0.05 unit/mL PNPase, which removes excess phosphate by converting it to ribose 1-phosphate as described previously (*33*, *36*, *37*). At these concentrations there was no competition between MDCC-PBP and the phosphate mop system for P_i. The MDCC fluorophore was excited at 425 nm, and fluorescence emission was detected at 465 nm. The relative fluorescence generated from MDCC-PBP was correlated to the concentration of P_i by a calibration curve where known concentrations of P_i were linearly increased and plotted versus the resulting change in fluorescent signal (data not shown). The observed rate constants were measured at varying concentrations of nucleotide from the linear region of initial velocity plots of P_i released over time. When plotted versus the concentration of nucleotide, both ATP and MANT-ATP yielded Michaelis−Menten kinetics as shown in Figure 1. This k_{cat}/K_m profile was performed in the absence and presence of S2 peptide for both ATP and MANT-ATP. The steady-state kinetic parameters are summarized in Table 1. Since the k_{cat}/K_m values are similar for MANT-ATP and ATP, we conclude that Lon hydrolyzes the fluorescent analogue in a comparable manner to ATP.

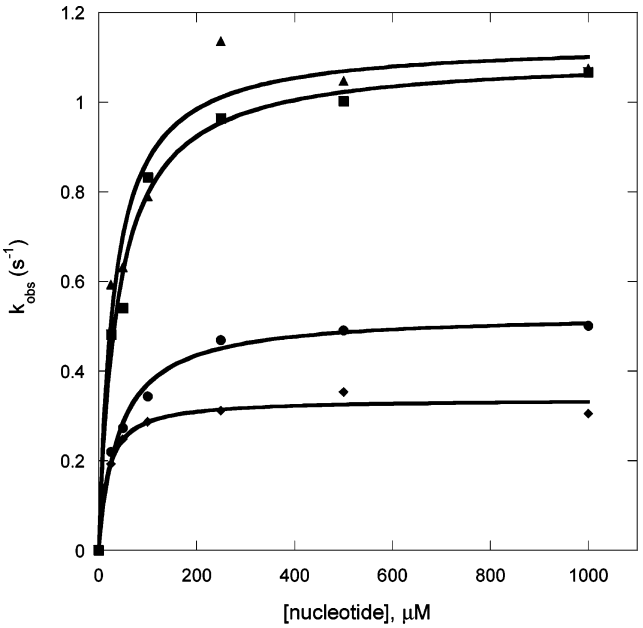

FIGURE 1: Steady-state kinetics of ATP and MANT-ATP hydrolysis by *E. coli* Lon. ATPase activity was monitored using a coupled assay system where MDCC-PBP binds the P_i released from the hydrolysis of ATP and MANT-ATP by Lon, resulting in an increase in fluorescence over time. The initial rates obtained from the time courses were converted to k_{obs} values by dividing the steady-state rates of the reactions by [Lon]. The (◆) and (▲) represent intrinsic and S2-stimulated ATPase activity, respectively, at varying concentrations of ATP. The (●) and (■) represent intrinsic and S2-stimulated MANT-ATPase activity, respectively, at varying concentrations of MANT-ATP. The data are reported as the average values of at least three trials and were fit with eq 1 to obtain the kinetic parameters k_{cat} and K_m. The kinetic parameters for intrinsic and S2-stimulated ATPase activity were $k_{cat} = 0.34 \pm 0.01$ s^{-1}, $K_m = 18 \pm 4$ μM (◆) and $k_{cat} = 1.1 \pm 0.1$ s^{-1}, $K_m = 31 \pm 8$ μM (▲), respectively. The kinetic parameters for intrinsic and S2-stimulated MANT-ATPase activity were $k_{cat} = 0.53 \pm 0.02$ s^{-1}, $K_m = 43 \pm 5$ μM (●) and $k_{cat} = 1.1 \pm 0.1$ s^{-1}, $K_m = 37 \pm 6$ μM (■), respectively. The rate constants are also summarized in Table 1.

Steady-State Analysis of MANT-ATP-Dependent S3 Cleavage by Lon. In addition to demonstrating that MANT-ATP is hydrolyzed by Lon protease, it was necessary to ensure that MANT-ATP was also capable of supporting S3 peptide cleavage in a comparable manner to ATP. The fluorescent peptidase assay previously employed to monitor the kinetics of ATP-mediated S3 cleavage (*25*, *27*, *30*) was performed to compare the ability of MANT-ATP to support S3 cleavage compared to ATP. The observed steady-state rate constants of S3 cleavage ($k_{ss,S3}$) were determined at varying concentrations of S3 (50−1500 μM) and 150 μM MANT-ATP or ATP. Because the predominant enzyme form under these conditions is Lon-ATP, the observed rate constants are a reflection of the effect of nucleotide hydrolysis rather than binding. The S3 hydrolysis reactions were monitored by the increase of fluorescence over time, which when calibrated reflects the amount of peptide hydrolyzed over time. The observed steady-state rate constants were then plotted as a function of S3 concentration, and this yielded a sigmoidal plot as shown in Figure 2. The kinetic parameters obtained from fitting the data in Figure 2 with the Hill equation are summarized in Table 2. Although the value of *n* determined here is slightly higher than that determined previously ($n = 1.6$), both are approximately equal to 2, and the discrepancy

Table 1: MANT-ATP and ATP Steady-State Kinetic Parameters Associated with ATP Hydrolysis

	intrinsic ATPase	intrinsic MANT-ATPase	S2-stimulated ATPase	S2-stimulated MANT-ATPase
k_{cat} (s^{-1})	0.34 ± 0.01	0.53 ± 0.02	1.1 ± 0.1	1.1 ± 0.1
K_m (μM)	18 ± 4	43 ± 5	31 ± 8	37 ± 6
k_{cat}/K_m ($10^3\ M^{-1}\ s^{-1}$)	19	12	35	30

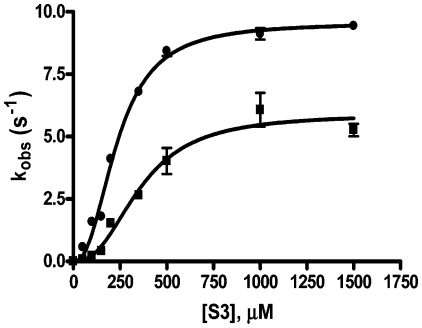

FIGURE 2: Steady-state kinetics of ATP- and MANT-ATP-dependent S3 cleavage by *E. coli* Lon. 150 μM ATP and MANT-ATP [5 mM $Mg(OAc)_2$] dependent peptidase activity was monitored using a modified FRET assay system where the cleavage of the S3 peptide containing a fluorescent donor and quencher results in donor/quencher separation and an increase in fluorescence over time. The initial steady-state rates of S3 cleavage were obtained from the time courses of peptide cleavage at varying [S3] and converted to steady-state rate constants $k_{ss,S3}$ by dividing by the [Lon]. Both ATP (●) and MANT-ATP (■) mediated S3 cleavage yielded sigmoidal curves which were fit with eq 2. The resulting kinetic parameters for ATP-mediated S3 cleavage (●) were $k_{ss,S3} = 9.6 \pm 0.2\ s^{-1}$, $K_{m,ATP} = 240 \pm 9\ \mu$M, and $n = 2.4 \pm 0.1$ while the parameters for MANT-ATP-mediated S3 cleavage were $k_{ss,S3} = 5.9 \pm 0.3\ s^{-1}$, $K_{m,MANT-ATP} = 360 \pm 30\ \mu$M, and $n = 2.5 \pm 0.4$. The rate constants are also summarized in Table 2.

Table 2: MANT-ATP and ATP Steady-State Kinetic Parameters Associated with S3 Cleavage

	$k_{ss,S3}$ (s^{-1})	K_m (μM)	*n*
ATP	9.6 ± 0.2	240 ± 9	2.4 ± 0.2
MANT-ATP	5.9 ± 0.3	360 ± 30	2.5 ± 0.4

is most likely due to the slightly differing experimental methods. Because the steady-state kinetic parameters were comparable to one another (Table 2), MANT-ATP supports S3 cleavage in a similar manner as ATP. In addition, these rate constants were comparable to the previously published k_{cat} and K_m values for ATP-mediated S3 cleavage (*25*, *30*). So although the nucleotide MANT-ATP contains a fluorescent label, it still supports S3 degradation in a similar manner to ATP and therefore is acceptable to use as an ATP analogue.

Limited Tryptic Digestion Probes the ATP-Dependent Conformational Change in Lon. Previously (*30*), we have utilized limited tryptic digestion to probe the functional role of nucleotide binding to Lon. This revealed an adenine-specific conformational change associated with nucleotide binding, which can primarily be monitored by the stability of a 67 kDa fragment of Lon. When sequenced, this fragment was composed of the ATPase, the substrate sensor and discriminatory domain (SSD), and protease domains of Lon. To ensure that the introduction of the fluorophore on MANT-ATP does not affect the nucleotide's ability to induce this conformational change in Lon, we subjected 1.4 μM Lon to limited tryptic digestion (1/50 w/w) in the presence of no

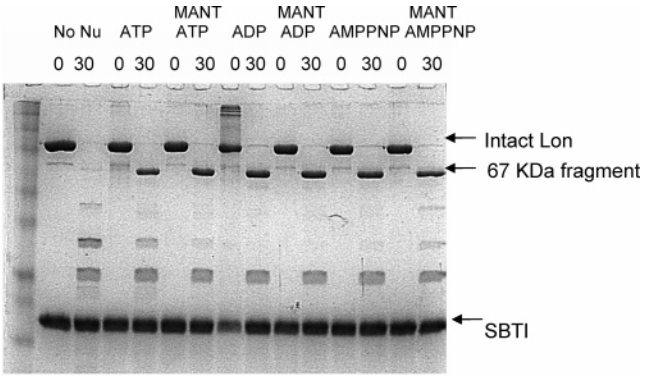

FIGURE 3: Limited tryptic digest shows that MANT-ATP and ATP induce the same conformational change in *E. coli* Lon protease. SDS−PAGE visualized by Coomassie brilliant blue show 1.4 μM Lon digested with a limiting amount of trypsin and quenched with SBTI at the indicated times as described in Materials and Methods. Lane 1 shows the molecular markers in kilodaltons (from top to bottom): 183, 114, 81, 64, 50, 37, 26, and 20. Lanes 2 and 3 contain Lon without nucleotide, lanes 4 and 5 contain Lon + 1 mM ATP, lanes 6 and 7 contain Lon + 1 mM MANT-ATP, lanes 8 and 9 contain Lon + 1 mM ADP, lanes 10 and 11 contain Lon + 1 mM MANT-ADP, lanes 12 and 13 contain Lon + 1 mM AMPPNP, and lanes 14 and 15 contain Lon + 1 mM MANT-AMPPNP.

nucleotide and saturating amounts (1 mM) of ATP, MANT-ATP, ADP, MANT-ADP, AMPPNP, and MANT-AMPPNP. At 0 and 30 min the reaction was quenched with soybean trypsin inhibitor (SBTI) and resolved on a 12.5% SDS−PAGE as shown in Figure 3. This figure demonstrates that MANT-ATP (lanes 4 and 5) induces the same conformational change as ATP (lanes 2 and 3). MANT-ADP (lanes 10 and 11) and MANT-AMPPNP (lanes 14 and 15) also induce the same conformational change as ADP (lanes 8 and 9) and AMPPNP (lanes 12 and 13) ,respectively. S2 peptide did not change the digestion pattern (data not shown), indicating that peptide does not induce any conformational change that is detectable by tryptic digestion.

Determining the Rate of MANT-ATP Binding Using Fluorescent Stopped Flow. Since MANT-ATP is hydrolyzed, supports peptide cleavage, and induces the same conformational change as ATP, the MANT−nucleotide fluorescent analogues can be used to study individual kinetic steps along the Lon reaction pathway. The on rate of MANT-ATP binding was monitored by stopped-flow fluorescence spectroscopy because an increase in fluorescence is detected upon Lon binding to MANT-ATP. Rapidly mixing 5 μM Lon both in the presence and in the absence of saturating amounts (500 μM) of S2 peptide with amounts of MANT-ATP varying from 1 μM to 100 μM resulted in time courses that were best fit using a double exponential equation. A representative time course is shown in Figure 4a with the solid black line demonstrating the fit of the double exponential equation (Materials and Methods). During the synthesis of MANT-ATP, the MANT fluorophore attaches to both the 2′- and 3′-hydroxyl on the ribose (*32*). The mixture

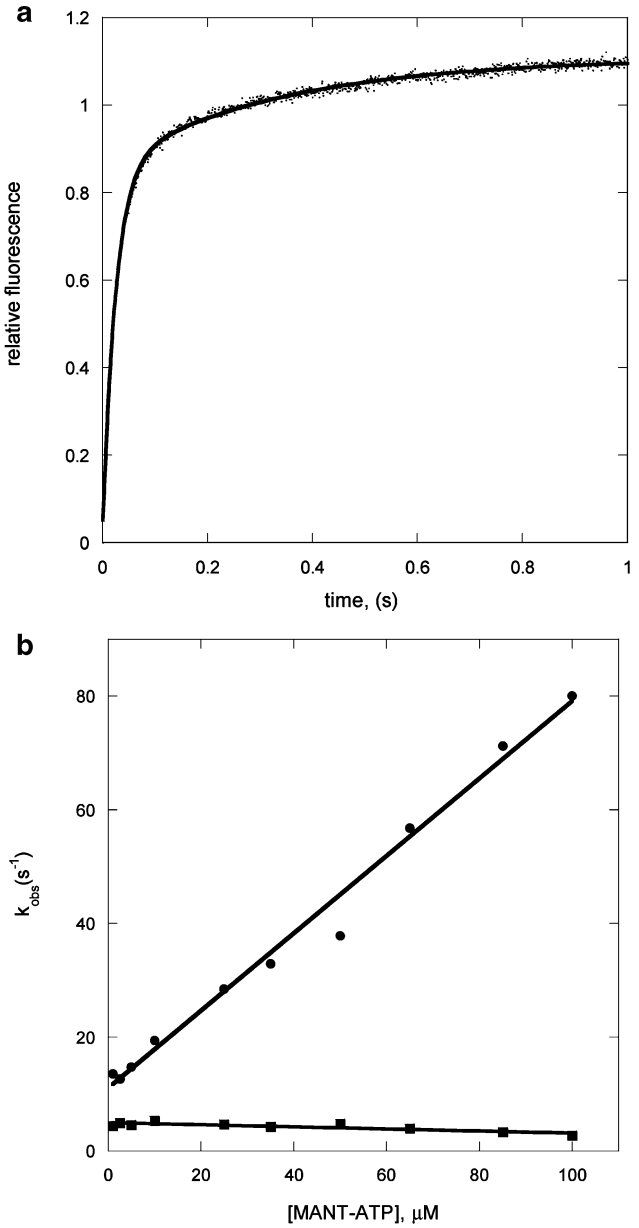

FIGURE 4: MANT-ATP binding to Lon. (a) Representative time course of MANT-ATP binding to Lon. Five micromolar Lon was rapidly mixed with varying amounts of MANT-ATP (excitation 360 nm, emission 450 nm) in the presence and absence of 500 μM S2 peptide, and the increase in fluorescence was monitored for 1 s. The time courses were fit with a double exponential (eq 3, solid black line). The two resulting rate constants ($k_{on,1}$, $k_{on,2}$) are shown in (b) at varying concentrations of MANT-ATP. (b) On-rate constants of MANT-ATP binding plotted versus [MANT-ATP]. $k_{on,1}$ shows a linear dependence on [MANT-ATP]. The on rate for MANT-ATP is determined from the slope of the line ($k_{on,MANT-ATP} = 6.8 \times 10^5$ M^{-1} s^{-1}). The off rate for MANT-ATP can be estimated from the *y*-intercept of the line ($k_{off,MANT-ATP} = 11$ s^{-1}). $k_{on,2}$ remains constant at 5 s^{-1}, likely indicating a conformational change associated with nucleotide binding. These rate constants are also summarized in Table 3.

of the two isomers could result in fluorescent changes which are unrelated to the enzyme nucleotide interaction. In order to ensure this was not the reason that biphasic time courses were observed, control experiments with MANT-dATP were performed which also resulted in biphasic time courses (data shown in Supporting Information). Two observed rate constants ($k_{on,1}$, $k_{on,2}$) are extracted from the double exponential equation and plotted versus the concentration of MANT-ATP as shown in Figure 4b. The rate constants associated with MANT-ATP binding are identical in the presence and absence of S2 peptide, indicating that peptide has no effect on the binding of nucleotide (Table 3). The data shown in Figure 4b are representative of MANT-ATP binding in the absence of S2. The observed rate constants, $k_{on,1}$, are linearly dependent on the concentration of MANT-ATP (Figure 4b). The slope of the line, 6.8×10^5 M^{-1} s^{-1}, yields the on rate of MANT-ATP binding, and the *y*-intercept is an estimate of the off rate (11 s^{-1}). Furthermore when the K_d is calculated by dividing the off rate by the on rate, the value (16 μM) is similar to the previously published value of 10 μM (*26*) for the low-affinity ATPase site (*28*). The range of nucleotide concentration needed to probe the high-affinity site (0.05−5 μM) was beyond the limit of detection at the lower concentrations and indistinguishable from the low-affinity site at the higher concentrations. The ATP off rate for the high-affinity ATPase site could not be detected using this method for the same reason. Instead, MANT-AMPPNP, a nonhydrolyzable analogue, was used as elaborated on in the Discussion. The observed rate constant, $k_{on,2} \sim 5$ s^{-1} (Figure 4b, Table 3), shows no dependence on the concentration of MANT-ATP. The lack of dependence on nucleotide concentration could be indicative of a conformational change step associated with MANT-ATP binding. This is supported by the tryptic digest which also suggests a conformational change upon nucleotide binding which protects Lon from degradation by trypsin (Figure 3) (*30*). The same binding experiment was conducted to determine the rate of MANT-ADP and MANT-AMPPNP binding to Lon, and the rate constants were comparable to MANT-ATP. The rate constant, $k_{on,2}$, did not vary with the concentration of nucleotide, which is again consistent with a conformational change (Table 3).

Table 3: Rate Constants Associated with Adenine Nucleotide Binding As Determined by Fluorescent Stopped Flow

MANT-nucleotide	$k_{on,MANT-Nu}$ (10^5 M^{-1} s^{-1})	$k_{off,MANT-Nu}$ (s^{-1})	$k_{on,2}$ (s^{-1})
ATP	6.8	11	4.1 ± 1.2
ATP + S2	6.8	10	3.7 ± 1.2
ADP	6.9	9.5 0.46[a] (0.13)[a]	3.9 ± 0.9
ADP + S2	6.1	9.7 0.44[a] (0.13)[a]	3.7 ± 0.9
AMPPNP	3.2	22 6.6[a] (0.16)[a]	6.7 ± 2.8
AMPPNP + S2	2.1	24 6.7[a] (0.16)[a]	7.1 ± 4.7

[a] Values determined by single mixing release rate experiments where Lon was preincubated with MANT nucleotide and then rapidly mixed with excess unlabeled nucleotide. These values are more accurate because the off rates are being directly measured in the experiment. Two off rates for the nucleotides are detected in this experiment. The off rate from the high-affinity site is in parentheses, and the other number represents the off rate from the low-affinity site.

Determining the Rate of MANT-ADP Release Using Fluorescent Stopped Flow. The rate constant associated with MANT-ADP release could also be monitored using fluorescence stopped-flow spectroscopy because there is a decrease in fluorescence upon the dissociation of MANT-ADP from Lon. Five micromolar Lon in the presence and absence of 500 μM S2 peptide was preincubated with 0.05−200 μM

MANT-ADP and rapidly mixed with excess unlabeled (1 mM) ADP. This resulted in a decrease in fluorescence which was best fit with a double exponential (Materials and Methods). A representative time course is shown in Figure 5a, where the solid black line represents the fit of the double exponential equation. To ensure that the two phases were not a result of esterification of the fluorophore on MANT-ATP, control experiments were performed using MANT-dADP which were also biphasic (data shown in Supporting Information). The two rate constants ($k_{off,1}$, $k_{off,2}$) obtained from the double exponential fit of the data are summarized in Table 4. As one would expect, there is no dependence on the concentration of MANT-ADP with either rate constant because the release step being monitored is a unimolecular event. The presence of S2 peptide also does not affect the rate constants associated with MANT-ADP release regardless of the order of addition. The average value for $k_{off,1}$ was 0.46 $\pm$ 0.03 s^{-1} and 0.14 $\pm$ 0.01 s^{-1} for $k_{off,2}$. To ensure that the MANT fluorescent label was not affecting the off rate, the experiment was also performed where Lon was preincubated with varying amounts of unlabeled ADP and rapidly mixed with MANT-ADP, resulting in an increase in fluorescence. The rate constants obtained from performing the experiment in this way were identical (data not shown), assuring that the fluorescent label was not affecting the observed rate constants. MANT-ADP release was also monitored by preincubating Lon with varying amounts of MANT-ATP for 30 min at 37 °C so all the MANT-ATP was hydrolyzed to MANT-ADP. The resulting mixture was then rapidly mixed with excess (1 mM) unlabeled ADP on the stopped flow. These resulting time courses were again identical to those where MANT-ADP was used directly (Table 4). This indicates that if by performing the experiments in this way we are indeed probing a pre- versus postcatalytic form of Lon, the two forms do not release MANT-ADP at differing rates. However, because there is not a clear mechanistic understanding of how Lon turns over, the possibility that we are isolating identical enzyme forms in the two experiments cannot be excluded.

The single mixing stopped-flow experiments discussed above are set up so that every fluorescent molecule bound to the enzyme is chased off. Because of the sensitivity of the stopped-flow method even at low concentrations of MANT-ADP the release rate from both sites was being detected (Table 4). Therefore, stopped-flow double mixing experiments were employed to uncouple MANT-ADP release from the high- and low-affinity ATPase sites. These experiments allowed for the mixing of two of the reaction components for a designated period of time prior to the introduction of the third component and subsequent monitoring of the fluorescent signal. We demonstrated in a previous publication that the high-affinity ATPase sites could be blocked by preincubating 6 μM Lon with stoichiometric amounts of ADP (*28*). Whether the ADP was generated in situ or directly added in the preincubation with Lon, the pre-steady-state ATP hydrolysis activity at the low-affinity sites remained unaffected. We utilized the high-affinity ATPase site blocking technique in this study to isolate MANT-ADP release from only the low-affinity site. To this end, 5 μM Lon preincubated with 5 μM ADP (saturates high-affinity sites) was rapidly mixed with 100 μM MANT-ADP (saturates low-affinity sites) for 3 ms. This reaction was subsequently mixed with 1 mM ADP $\pm$ 500 μM S2 and the decrease in fluorescence monitored as in the above experiments. The same experiment was performed with 100 μM

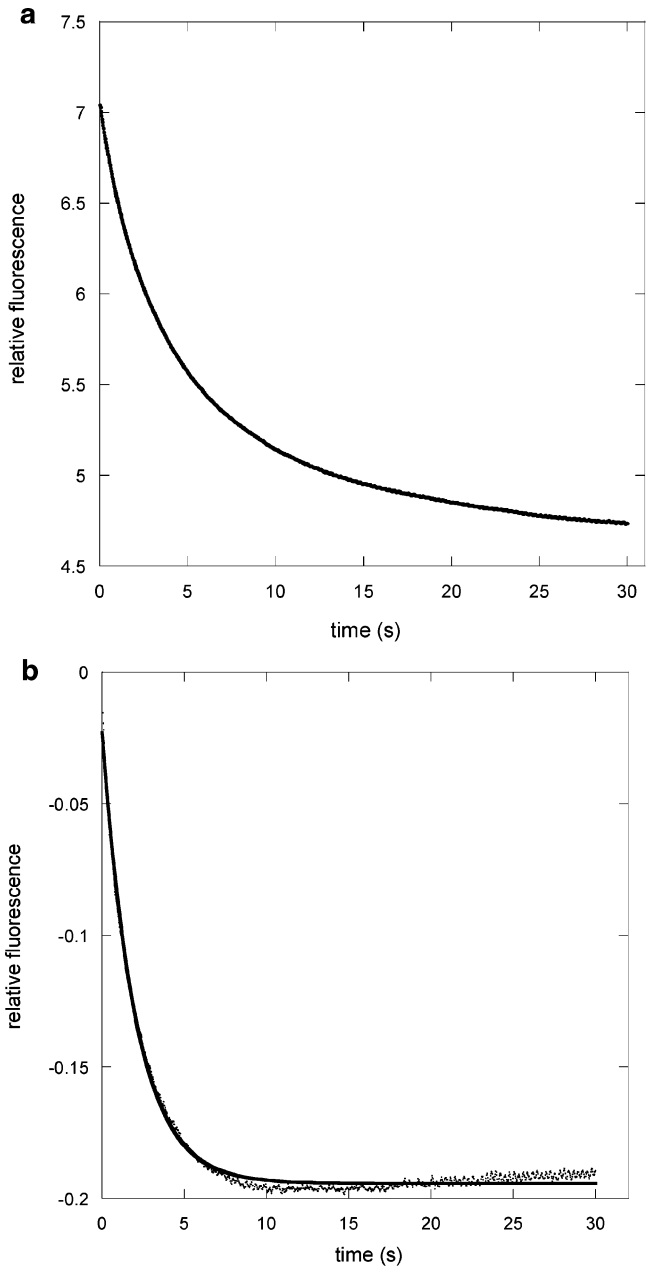

FIGURE 5: MANT-ADP release from Lon. (a) Representative time course of MANT-ADP release in single mixing experiments. Five micromolar Lon was preincubated with varying amounts of MANT-ADP or MANT-ATP (excitation 360 nm, emission 450 nm) in the presence and absence of 500 μM S2 peptide and rapidly mixed with 1 mM ADP. The resulting decrease in fluorescence was monitored for 30 s, and the time courses were fit with a double exponential (eq 3, solid black line). Two averaged rate constants, $k_{off,1}$ = 0.46 $\pm$ 0.03 s^{-1} and $k_{off,2}$ = 0.14 $\pm$ 0.01 s^{-1}, resulted and are summarized in Table 4. (b) Representative time course of ADP release in double mixing experiments. The high-affinity ATPase sites in 5 μM Lon were blocked with 5 μM ADP, and this mixture was rapidly mixed with 100 μM MANT-ADP or MANT-ATP for 3 ms or 50 s, respectively. 1 mM ADP then mixes with the reaction to displace the bound nucleotide, and the decrease in fluorescence is monitored for 30 s. The time courses were fit with a single exponential equation (solid black line), and the resulting rate constant ($k_{off,1}$ = 0.5 $\pm$ 0.1 s^{-1}) describes the release of ADP from only the low-affinity sites.

Table 4: Summary of MANT-ADP Release Rate Constants from Single Mixing Stopped-Flow Experiments

	intrinsic $k_{off,1}$ (s^{-1})		S2-stimulated $k_{off,1}$ (s^{-1})		intrinsic $k_{off,2}$ (s^{-1})		S2-stimulated $k_{off,2}$ (s^{-1})	
[MANT-Nu] (μM)	MANT-ADP	MANT-ATP	MANT-ADP	MANT-ATP	MANT-ADP	MANT-ATP	MANT-ADP	MANT-ATP
0.05	0.42 ± 0.01	0.43 ± 0.01	0.45 ± 0.01	0.44 ± 0.01	0.12 ± 0.01	0.12 ± 0.01	0.12 ± 0.01	0.12 ± 0.01
0.1	0.52 ± 0.01	0.44 ± 0.01	0.45 ± 0.01	0.46 ± 0.02	0.13 ± 0.01	0.13 ± 0.02	0.13 ± 0.01	0.14 ± 0.02
0.5	0.47 ± 0.02	0.51 ± 0.16	0.47 ± 0.02	0.46 ± 0.02	0.15 ± 0.01	0.13 ± 0.02	0.15 ± 0.01	0.14 ± 0.02
50	0.42 ± 0.01	0.46 ± 0.04	0.45 ± 0.01	0.49 ± 0.05	0.12 ± 0.01	0.12 ± 0.04	0.12 ± 0.01	0.13 ± 0.04
200	0.46 ± 0.06	ND[a]	0.40 ± 0.04	ND	0.14 ± 0.01	ND	0.14 ± 0.01	ND
				0.44 ± 0.01	0.12 ± 0.01	0.12 ± 0.01	0.12 ± 0.01	0.12 ± 0.01

[a] ND: these values were not determined.

MANT-ATP except the delay time was increased to 50 s to allow for complete hydrolysis of MANT-ATP at the low-affinity sites. Figure 5b illustrates a representative time course from the double mixing experiments. The time course is single exponential in nature presumably because MANT-ADP release from only the low-affinity sites is being monitored. The solid black line shows the fit of a single exponential equation resulting in a rate constant of $0.5 \pm 0.1\ s^{-1}$ for ADP release at the low-affinity sites. By inference, the second rate constant detected in the single mixing experiments ($k_{off,2} = 0.14\ s^{-1}$, Figure 5a, Table 4) must describe the release of ADP from the high-affinity ATPase site.

DISCUSSION

Lon is a homohexameric ATP-dependent protease in which the ATPase and protease domains are located within each enzyme subunit. Using MANT−nucleotides as fluorescent probes, we were able to compare the kinetics of ATP, AMPPNP, and ADP binding to and release from *E. coli* Lon. The pre-steady-state binding experiments performed in this study verified that the on rate of ATP binding is comparable to AMPPNP and that a conformational change occurs after nucleotide binding (Table 3). Therefore, the difference between ATP- and AMPPNP-activated peptide cleavage occurs after nucleotide binding. Although there is only one ATP binding domain on each monomeric subunit in Lon, studies have identified two binding affinities for ATP ($K_{d,low\ affinity} = 10\ \mu M$, $K_{d,high\ affinity} < 1\ \mu M$) (*26*). Additional experiments performed in this laboratory isolated the binding constant at the high-affinity site to be $0.52 \pm 0.02\ \mu M$ (*28*). When the hydrolysis activity of each ATPase site was examined using single turnover experiments, the high-affinity sites were found to hydrolyze ATP very slowly ($0.01\ s^{-1}$) (*28*). The ATP binding experiments performed in the present study encompassed a range of ATP concentrations that included both the high- and low-affinity sites. Both sites were found to have a similar on rate which is relatively fast (Table 3). Therefore, because the dissociation constant, K_d, is defined by k_{off}/k_{on}, the high-affinity ATPase site must have a slower k_{off} than the low-affinity site. The value $10\ s^{-1}$ obtained from the *y*-intercept of Figure 4b (Table 3) yields an estimate of the k_{off} of ATP for the low-affinity site. This method was not sensitive enough to distinguish a second value for the high-affinity sites because the off rate is not being directly measured in the experiment. Instead, MANT-AMPPNP was used as a probe because it is a nonhydrolyzable analogue of ATP which supports S2 peptide cleavage and displays identical binding kinetics to Lon as MANT-ATP. The off rate could then be directly monitored using the same methodology used for detecting the k_{off} for MANT-ADP. Two observed rate constants for MANT-AMPPNP release resulted, which did not vary in the presence of S2 peptide (Table 3). When the observed off rates were divided by the on rate, the two K_d values obtained for AMPPNP were 0.3 and 9 μM. These values are in close agreement with the K_d values of the high- and low-affinity ATPase sites determined previously [0.5 μM (*28*), 10 μM (*26*)]. Therefore, it is likely that the k_{off} values of ATP are the same as AMPPNP.

To characterize the kinetics of ADP interacting with Lon, we utilized single mixing stopped-flow experiments to determine the off rate of MANT-ADP, which resulted in two observed rate constants ($k_{off,1} = 0.46 \pm 0.03\ s^{-1}$, $k_{off,2} = 0.14 \pm 0.01\ s^{-1}$, Table 4). However, only one rate constant associated with the binding of ADP which is dependent on the concentration of nucleotide was detected ($6.9 \times 10^5\ M^{-1}\ s^{-1}$, Table 3). The difference between the two observed ADP off rates is modest so when the off rates are divided by the on rate, it yields two K_d values that differ only by 3-fold. Since the original article that investigated the binding of nucleotides to Lon had a detection limit of 1 μM for ATP binding (*26*), it is not surprising that a subtle difference in the K_d for ADP was not detected in the nanomolar range. Furthermore, when the double mixing experiment was performed with MANT-ATP, if the delay time was not long enough to allow for complete hydrolysis of MANT-ATP at the low-affinity site (Figure 1, $0.5\ s^{-1}$), the off rate of MANT-ATP as well as MANT-ADP was detected. As the high-affinity ATPase site hydrolyzes ATP much more slowly [$0.01\ s^{-1}$ (*28*)] than the low-affinity site (Figure 1, $0.5\ s^{-1}$), it is likely that ADP release at the high-affinity site occurs much later than at the low-affinity site.

Kinetic studies performed previously indicated that ADP release was the rate-limiting step along the reaction pathway of Lon protease (*26*, *27*, *38*). This conclusion was supported by a proposed ATP/ADP exchange model which was based on data that showed that Lon was proteolytically "inactive" when bound to ADP, that protein substrate allosterically interacted with Lon to promote ADP release which was the rate-limiting step, and that Lon was only proteolytically "active" when the bound ADP was exchanged to ATP (*38*). The fact that nonhydrolyzable analogues such as AMPPNP, which does not generate ADP, support peptide cleavage at a lower rate than ATP negates this proposed model. The kinetic mechanism has been further investigated recently using pre-steady-state kinetic techniques to determine the timing of events along the pathway. ATP hydrolysis was found to occur prior to peptide cleavage at the low-affinity site (*25*, *27*). Because burst kinetics was detected in the pre-

steady-state time course of ATP hydrolysis, the rate-limiting step must occur after ATP hydrolysis, and ADP release would be consistent with this. The rate-limiting step should also have a rate constant similar to the overall k_{cat} for ATP hydrolysis. As shown in Figure 1, the k_{cat} for S2-stimulated ATP hydrolysis is 1.1 and 0.53 s^{-1} for intrinsic ATP hydrolysis. We have previously suggested that the S2 stimulation of the steady-state ATPase activity is a result of the high-affinity sites interacting with peptide (*28*). Because both of the rate constants identified in this study for MANT-ADP release were slower than the S2-stimulated k_{cat} for ATP hydrolysis, we questioned the validity of this suggestion. When the timing of all of the pre-steady-state experiments was examined in entirety, the high-affinity sites seem to be essentially catalytically inactive. Prior pulse−chase (*27*) and single turnover (*28*) experiments demonstrate that the high-affinity ATPase site is capable of hydrolyzing ATP if given enough time; however, the steady-state rate is never affected by the high-affinity ATPase activity. Furthermore, although Lon (5 μM) undergoes multiple rounds of peptide cleavage at limiting (500 nM) ATP, 100 μM peptide is cleaved prior to the half-life of the high-affinity ATPase site reaction (*28*). For these reasons it appears that the ATPase pre-steady-state burst activity as well as the steady-state activity can be attributed to the low-affinity sites. However, a detailed understanding of how the S2 peptide is interacting with Lon to stimulate steady-state ATPase activity is still necessary. The steady-state k_{cat} values can thus be attributed to low-affinity ATPase activity which is stimulated in the presence of peptide. Because the off rate of MANT-ADP from the low-affinity site (0.46 s^{-1}, Table 4) approaches the turnover number for intrinsic MANT-ATPase activity (0.53 s^{-1}, Table 1), ADP release is likely the rate-limiting step in this pathway. Prior experiments have been performed which suggested that the presence of peptide or protein substrate facilitated the release of ADP from Lon. Menon and Goldberg demonstrated this in two ways. After incubation with [^{3}H]ADP to establish an equilibrium the addition of casein to the reaction resulted in the recovery of lesser amounts of [^{3}H]ADP−Lon complex over time than in the absence of casein (*38*). They also noted that basal ATP hydrolysis was inhibited by a greater percentage in the absence versus the presence of casein (*38*). Thomas-Wohlever and Lee confirmed these observations using steady-state ADP inhibition analyses of ATP-dependent S3 cleavage by Lon protease. They measured K_{is} and K_{ii} values which reflected affinity of Lon for ADP in the presence of very low and high levels of S3, respectively. The affinity for ADP was weakened in the presence of higher levels of S3 ($K_{ii} > K_{is}$) presumably by binding allosterically to promote ADP/ATP exchange (*25*). Collectively, these results would suggest that the rate of ADP release is possibly increased in the presence of peptide or protein substrate. However, the results of the stopped-flow MANT-ADP release experiments summarized in Table 4 demonstrate that there is no difference in the off rate in the presence of peptide (Table 4) or protein substrate (data not shown). The rate constant for ATP binding and the conformational change detected upon nucleotide binding were also unaffected by peptide or protein substrate (Table 3). As no pre-steady-state rate constant identified thus far has been affected by S2 peptide, we therefore conclude that the obtained pre-steady-state rate constants describe the first round of ATP hydrolysis which is independent of peptide. If peptide is present, it acts on a enzyme form following the first round of ATP hydrolysis which is then catalytically active and described by the peptide stimulated k_{cat} (1 s^{-1}, Table 1). Further experimentation will have to be performed to isolate the intermediates in this pathway.

Scheme 1[a]

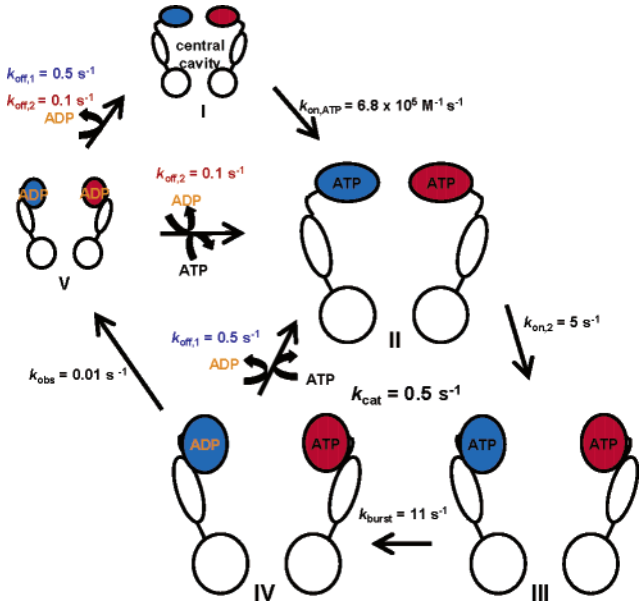

[a] Form I represents oligomeric free enzyme shown for simplicity as a dimer (bottom white circle = peptidase domain, middle white oval = substrate senor and discriminatory domain (SSD), top left blue oval = low-affinity ATPase, and top right red oval = high-affinity ATPase). Forms II−IV represent intrinsic steady-state ATPase activity at the low-affinity sites. Form V represents the ability of the high-affinity site to hydrolyze ATP.

The best estimate of a turnover number for the high-affinity sites is 0.01 s^{-1}, as demonstrated using single turnover methods described previously (*28*). However, the high-affinity ATPase sites release ADP at 0.14 s^{-1}, which is faster than the turnover number (0.01 s^{-1}). Thus another step must be limiting turnover at the high-affinity site. Until the activities at the two sites can be more easily uncoupled this step will likely remain unknown. However, because hydrolysis is so slow and appears to not contribute to the ATP-dependent peptidase activity of Lon, it would not be surprising if chemistry or a step prior to chemistry was rate limiting for the high-affinity site.

An additional step along the pathway that we attempted to monitor was the release of phosphate (P_i) from Lon. The MDCC-PBP fluorescent coupled assay system used to monitor the steady-state hydrolysis of MANT-ATP is the ideal way to approach this. Unfortunately, the production of P_i in the pre-steady-state was below the detection limit of the MDCC-PBP method under our assay conditions. Phosphate release has been proposed to be negligible because increasing amounts of phosphate do not inhibit the activity of Lon (*25*) and P_i was never found to remain bound to Lon as ADP was in equilibrium binding experiments (*26*, *38*).

In summary, we have utilized pre-steady-state techniques to determine the kinetic mechanism of the ATPase activities of Lon. Collectively, our results allow us to refine the previously constructed kinetic mechanism of *E. coli* Lon (*25*, *27*). The revised model is illustrated in Scheme 1 in the

Scheme 2[a]

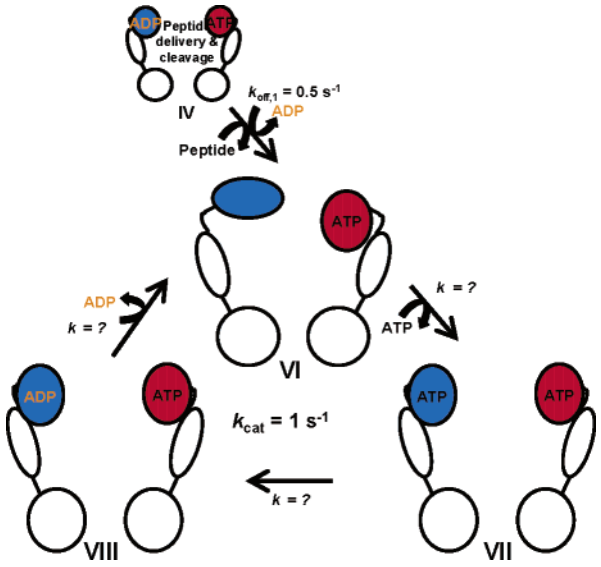

[a] As in Scheme 1, in form IV Lon has hydrolyzed the first round of ATP at the low-affinity sites. Following ADP release from the low-affinity ATPase site after the first turnover, if peptide substrate is present, we propose enzyme forms VI and VII.

absence of peptide, and then Scheme 2 proposes a kinetic model for ATPase activity in the presence of peptide. Although Lon exists as a higher order oligomer shown in partial crystal structures as a hexamer (*15*, *16*, *39*), we represent it as a dimer in order to simplify the schemes. Each Lon monomer contains four defined domains, the amino terminus, ATPase, substrate sensor and discriminatory (SSD), and the protease domain. The amino terminus is not represented in the schemes for simplicity, the low-affinity ATPase domains are represented as blue ovals, the high-affinity ATPase domains are represented as red ovals, the SSD domain is represented as white ovals, and the peptidase domain is represented as white circles. In Scheme 1, Lon in its free enzyme (form I) binds to ATP at both the high- and low-affinity ATPase sites at a fast rate (Table 3, $k_{on,ATP}$ = 6.8 × 10^5 M^{-1} s^{-1}). The binding of nucleotide induces a conformational change (form II) (*25*) measured in the stopped-flow binding experiments at approximately 5 s^{-1} (Table 3). ATP is subsequently hydrolyzed at the low-affinity ATPase sites at 11 s^{-1} (form IV) (*27*, *28*), and ADP is released from the low-affinity ATPase sites at 0.5 s^{-1} (Table 4). Turnover at the low-affinity ATPase sites then occurs in the absence of peptide (forms II−IV) (Table 1, k_{cat} = 0.5 s^{-1}) and is limited by ADP release. In a separate pathway (forms IV and V) the high-affinity ATPase sites can hydrolyze ATP at 0.01 s^{-1} (*28*) and release ADP at 0.1 s^{-1} (Table 4).

Scheme 2 represents the proposed kinetic mechanism for ATPase activity in the presence of peptide. On the basis that peptide affects only the steady-state ATPase activity of the low-affinity sites, we propose that Lon adopts a different form after its first turnover as an ATP-dependent protease, i.e., from IV to VI. Enzyme form VI is speculative, although previous tryptic digest studies tentatively support its existence (*28*). Catalytic steady-state turnover can then occur (forms VI−VIII) as described by the peptide-stimulated k_{cat} = 1 s^{-1} (Table 1). The individual steps along this pathway will need to be defined in the future but will depend on the ability

Scheme 3[a]

$$E+A \underset{k_{-1}}{\overset{k_{+1}}{\rightleftharpoons}} EA \underset{k_{-2}}{\overset{k_{+2}}{\rightleftharpoons}} FP \underset{k_{-3}}{\overset{k_{+3}}{\rightleftharpoons}} F+P \rightleftharpoons A+F \underset{k_{-4}}{\overset{k_{+4}}{\rightleftharpoons}} FA \underset{k_{-5}}{\overset{k_{+5}}{\rightleftharpoons}} FQ \underset{k_{-6}}{\overset{k_{+6}}{\rightleftharpoons}} F+Q$$

k_{+1} = 0.7 μM^{-1} s^{-1} k_{+4} = 10 μM^{-1} s^{-1}
k_{-1} = 7 s^{-1} k_{-4} = 5 s^{-1}
k_{+2} = 8 s^{-1} k_{+5} = 50 μM s^{-1}
k_{+3} = 0.5 s^{-1} k_{+6} = 5 s^{-1}
k_{-3} = 1 μM^{-1} s^{-1} k_{-6} = 5 μM^{-1} s^{-1}

[a] E and F are different catalytic forms of Lon along the reaction pathway.

Table 5: Comparison of Experimentally Obtained Rate Constants with Those Determined from the Collective Fit of the Data to the Kinetic Mechanism in Scheme 3

	FitSim value	exptl value
k_{+1} (μM^{-1} s^{-1})	0.7	0.7
k_{-1} (s^{-1})	7	7
k_{+2} (s^{-1})	8	11[a]
k_{+3} (s^{-1})	0.5	0.5
k_{-3} (μM^{-1} s^{-1})	1	0.6
k_{+4} (μM^{-1} s^{-1})	10	ND[b]
k_{-4} (s^{-1})	5	ND[b]
k_{+5} (μM^{-1} s^{-1})	50	ND[b]
k_{+6} (s^{-1})	5	ND[b]
k_{-6} (μM^{-1} s^{-1})	5	ND[b]

[a] Values obtained from ref *27*. [b] Values have yet to be experimentally determined.

to isolate enzyme form VI to study using pre-steady-state techniques. Peptide could still be interacting with enzyme form VII to promote ADP release, which would be consistent with the observations proposed in the steady-state studies. The details concerning exactly how the peptide is interacting with the enzyme in this pathway will also need to be further defined and are thus shown only as "peptide delivery & cleavage" in Scheme 2. We have previously shown that the pre-steady-state peptide hydrolysis exhibits lag kinetics (*27*). Although no definitive evidence exists, we have proposed that the lag is an ATP-dependent translocation step (*27*). In order to probe the validity of this proposal, the microscopic rate constants associated with peptide binding, delivery, and cleavage are currently being investigated.

Previously, we reported a sequential ATP hydrolysis reaction model to account for the functional nonequivalency detected in the two ATPase sites in Lon (*27*). This model assumed that ATP occupancy at the low-affinity sites promoted the subsequent hydrolysis of ATP at the high-affinity sites. Further experimentation revealed that the hydrolysis of the two ATPase sites appeared independent of one another and that the pre-steady-state burst in ADP production could be attributed solely to low-affinity ATPase site activity (*28*). In light of the results obtained in this work and in previous single turnover experiments, we have revised the former kinetic model for the low-affinity ATPase sites as shown in Scheme 3. To check for consistency between the revised model and the S2-stimulated ATP hydrolysis reaction time courses that were reported previously, we collectively re-fit the data to the revised mechanism by regression analysis using FitSim (*40*−*42*). The results are summarized in Table 5 and Figure 6. As the burst amplitude but not the burst rate constants of the time courses varied with [ATP], we input the burst amplitude values determined

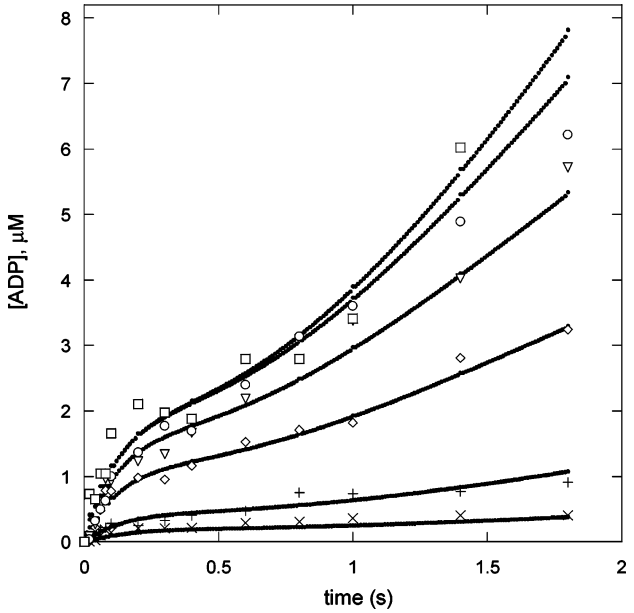

FIGURE 6: Collective fit of acid-quench ATPase data from ref *27* using FitSim. Simulation of the ATPase mechanism outlined in Scheme 3 was performed using FitSim. The resulting solid lines yielded the rate constants summarized in Scheme 3 and Table 5 and were overlaid with the experimental data from ref *27* for ATP hydrolysis. This demonstrates consistency with the proposed sequential mechanism. The experimental time courses represent the hydrolysis of [α-^{32}P]ATP as determined using an acid quench experiment at (×) 5 μM ATP, (+) 10 μM ATP, (◇) 25 μM ATP, (▽) 50 μM ATP, (○) 100 μM ATP, and (□) 200 μM ATP.

previously as the specified enzyme concentration for the corresponding [ATP] in the fitting process. In Scheme 3, the enzyme form F represents only the low-affinity ATPase sites and corresponds to the graphical enzyme for IV depicted in Schemes 1 and 2. It is discernible from Figure 6 that the kinetic data overlay well with the fitted time courses and from Table 5 that the theoretical rate constants agree closely with those obtained experimentally. It should be noted that although the hydrolytic activities of the high- and low-affinity sites are independent of one another, it is possible that the binding of ATP to the high-affinity sites may still have an effect on ATP binding to the low-affinity sites such that only the burst amplitude but not the burst rates of ATP hydrolysis at the low-affinity sites are affected. The kinetic experiments reported in this study cannot resolve this issue, and experiments beyond kinetics may be needed to further address this issue.

ACKNOWLEDGMENT

We thank Hilary Frase for aid in cloning phosphate binding protein and Jessica Ward for careful reading of the manuscript.

SUPPORTING INFORMATION AVAILABLE

ATP binding and release experiments were performed using MANT-dATP and MANT-dADP, respectively. The deoxyribonucleotides were used in order to ensure that the biphasic nature of the time courses was not a result of esterification of the fluorophore on the ribonucleotides MANT-ATP and MANT-ADP. Representative biphasic time courses of MANT-dATP binding and MANT-dADP release are shown. This material is available free of charge via the Internet at http://pubs.acs.org.

REFERENCES

1. Charette, M. F., Henderson, G. W., Doane, L. L., and Markovitz, A. (1984) DNA-stimulated ATPase activity on the lon (CapR) protein, *J. Bacteriol. 158*, 195−201.
2. Chung, C. H., and Goldberg, A. L. (1981) The product of the lon (capR) gene in Escherichia coli is the ATP-dependent protease, protease La, *Proc. Natl. Acad. Sci. U.S.A. 78*, 4931−4935.
3. Goff, S. A., and Goldberg, A. L. (1985) Production of abnormal proteins in E. coli stimulates transcription of lon and other heat shock genes, *Cell 41*, 587−595.
4. Goldberg, A. L., Moerschell, R. P., Chung, C. H., and Maurizi, M. R. (1994) ATP-dependent protease La (lon) from Escherichia coli, *Methods Enzymol. 244*, 350−375.
5. Goldberg, A. L., and Waxman, L. (1985) The role of ATP hydrolysis in the breakdown of proteins and peptides by protease La from Escherichia coli, *J. Biol. Chem. 260*, 12029−12034.
6. Gottesman, S. (1996) Proteases and their targets in Escherichia coli, *Annu. Rev. Genet. 30*, 465−506.
7. Gottesman, S., Gottesman, M., Shaw, J. E., and Pearson, M. L. (1981) Protein degradation in E. coli: the Ion mutation and bacteriophage lambda N and cll protein stability, *Cell 24*, 225−233.
8. Gottesman, S., and Maurizi, M. R. (1992) Regulation by proteolysis: energy-dependent proteases and their targets, *Microbiol. Rev. 56*, 592−621.
9. Maurizi, M. R. (1992) Proteases and protein degradation in Escherichia coli, *Experientia 48*, 178−201.
10. Schoemaker, J. M., Gayda, R. C., and Markovitz, A. (1984) Regulation of cell division in Escherichia coli: SOS induction and cellular location of the sulA protein, a key to lon-associated filamentation and death, *J. Bacteriol. 158*, 551−561.
11. Neuwald, A. F., Aravind, L., Spouge, J. L., and Koonin, E. V. (1999) AAA+: A class of chaperone-like ATPases associated with the assembly, operation, and disassembly of protein complexes, *Genome Res. 9*, 27−43.
12. Ogura, T., and Wilkinson, A. J. (2001) AAA+ superfamily ATPases: common structure−diverse function, *Genes Cells 6*, 575−597.
13. Suzuki, C. K., Suda, K., Wang, N., and Schatz, G. (1994) Requirement for the yeast gene LON in intramitochondrial proteolysis and maintenance of respiration, *Science 264*, 891.
14. Botos, I., Melnikov, E. E., Cherry, S., Khalatova, A. G., Rasulova, F. S., Tropea, J. E., Maurizi, M. R., Rotanova, T. V., Gustchina, A., and Wlodawer, A. (2004) Crystal structure of the AAA+ alpha domain of E. coli Lon protease at 1.9Å resolution, *J. Struct. Biol. 146*, 113−122.
15. Botos, I., Melnikov, E. E., Cherry, S., Tropea, J. E., Khalatova, A. G., Rasulova, F., Dauter, Z., Maurizi, M. R., Rotanova, T. V., Wlodawer, A., and Gustchina, A. (2004) The catalytic domain of Escherichia coli Lon protease has a unique fold and a Ser-Lys dyad in the active site, *J. Biol. Chem. 279*, 8140−8148.
16. Rudyak, S. G., Brenowitz, M., and Shrader, T. E. (2001) Mg^{2+}-linked oligomerization modulates the catalytic activity of the Lon (La) protease from Mycobacterium smegmatis, *Biochemistry 40*, 9317−9323.
17. van Dijl, J. M., Kutejova, E., Suda, K., Perecko, D., Schatz, G., and Suzuki, C. K. (1998) The ATPase and protease domains of yeast mitochondrial Lon: roles in proteolysis and respiration-dependent growth, *Proc. Natl. Acad. Sci. U.S.A. 95*, 10584−10589.
18. Matsui, H., Suzuki, M., Isshiki, Y., Kodama, C., Eguchi, M., Kikuchi, Y., Motokawa, K., Takaya, A., Tomoyasu, T., and Yamamoto, T. (2003) Oral immunization with ATP-dependent protease-deficient mutants protects mice against subsequent oral challenge with virulent Salmonella enterica serovar typhimurium, *Infect. Immun. 71*, 30−39.
19. Takaya, A., Suzuki, M., Matsui, H., Tomoyasu, T., Sashinami, H., Nakane, A., and Yamamoto, T. (2003) Lon, a stress-induced ATP-dependent protease, is critically important for systemic Salmonella enterica serovar typhimurium infection of mice, *Infect. Immun. 71*, 690−696.
20. Takaya, A., Tomoyasu, T., Tokumitsu, A., Morioka, M., and Yamamoto, T. (2002) The ATP-dependent lon protease of Salmonella enterica serovar Typhimurium regulates invasion and

expression of genes carried on Salmonella pathogenicity island 1, *J. Bacteriol. 184*, 224−232.
21. Robertson, G. T., Kovach, M. E., Allen, C. A., Ficht, T. A., and Roop, R. M., 2nd. (2000) The Brucella abortus Lon functions as a generalized stress response protease and is required for wild-type virulence in BALB/c mice, *Mol. Microbiol. 35*, 577−588.
22. Losada, L. C., and Hutcheson, S. W. (2005) Type III secretion chaperones of Pseudomonas syringae protect effectors from Lon-associated degradation, *Mol. Microbiol. 55*, 941−953.
23. Maurizi, M. R. (1987) Degradation in vitro of bacteriophage lambda N protein by Lon protease from Escherichia coli, *J. Biol. Chem. 262*, 2696−2703.
24. Lee, I., and Berdis, A. J. (2001) Adenosine triphosphate-dependent degradation of a fluorescent lambda N substrate mimic by Lon protease, *Anal. Biochem. 291*, 74−83.
25. Thomas-Wohlever, J., and Lee, I. (2002) Kinetic characterization of the peptidase activity of Escherichia coli Lon reveals the mechanistic similarities in ATP-dependent hydrolysis of peptide and protein substrates, *Biochemistry 41*, 9418−9425.
26. Menon, A. S., and Goldberg, A. L. (1987) Binding of nucleotides to the ATP-dependent protease La from Escherichia coli, *J. Biol. Chem. 262*, 14921−14928.
27. Vineyard, D., Patterson-Ward, J., Berdis, A. J., and Lee, I. (2005) Monitoring the timing of ATP hydrolysis with activation of peptide cleavage in Escherichia coli Lon by transient kinetics, *Biochemistry 44*, 1671−1682.
28. Vineyard, D., Patterson-Ward, J., and Lee, I. (2006) Single-turnover kinetic experiments confirm the existence of high- and low-affinity ATPase sites in Escherichia coli Lon protease, *Biochemistry 45*, 4602−4610.
29. Chung, C. H., and Goldberg, A. L. (1982) DNA stimulates ATP-dependent proteolysis and protein-dependent ATPase activity of protease La from Escherichia coli, *Proc. Natl. Acad. Sci. U.S.A. 79*, 795−799.
30. Patterson, J., Vineyard, D., Thomas-Wohlever, J., Behshad, R., Burke, M., and Lee, I. (2004) Correlation of an adenine-specific conformational change with the ATP-dependent peptidase activity of Escherichia coli Lon, *Biochemistry 43*, 7432−7442.
31. Jameson, D. M., and Eccleston, J. F. (1997) Fluorescent nucleotide analogs: synthesis and applications, *Methods Enzymol. 278*, 363−390.
32. Hiratsuka, T. (1983) New ribose-modified fluorescent analogs of adenine and guanine nucleotides available as substrates for various enzymes, *Biochim. Biophys. Acta 742*, 496−508.
33. Brune, M., Hunter, J. L., Corrie, J. E., and Webb, M. R. (1994) Direct, real-time measurement of rapid inorganic phosphate release using a novel fluorescent probe and its application to actomyosin subfragment 1 ATPase, *Biochemistry 33*, 8262−8271.
34. Lionne, C., Brune, M., Webb, M. R., Travers, F., and Barman, T. (1995) Time resolved measurements show that phosphate release is the rate limiting step on myofibrillar ATPases, *FEBS Lett. 364*, 59−62.
35. Medveczky, N., and Rosenberg, H. (1969) The binding and release of phosphate by a protein isolated from Escherichia coli, *Biochim. Biophys. Acta 192*, 369−371.
36. Brune, M., Hunter, J. L., Howell, S. A., Martin, S. R., Hazlett, T. L., Corrie, J. E., and Webb, M. R. (1998) Mechanism of inorganic phosphate interaction with phosphate binding protein from Escherichia coli, *Biochemistry 37*, 10370−10380.
37. Webb, M. R. (1992) A continuous spectrophotometric assay for inorganic phosphate and for measuring phosphate release kinetics in biological systems, *Proc. Natl. Acad. Sci. U S.A. 89*, 4884−4887.
38. Menon, A. S., and Goldberg, A. L. (1987) Protein substrates activate the ATP-dependent protease La by promoting nucleotide binding and release of bound ADP, *J. Biol. Chem. 262*, 14929−14934.
39. Park, S. C., Jia, B., Yang, J. K., Van, D. L., Shao, Y. G., Han, S. W., Jeon, Y. J., Chung, C. H., and Cheong, G. W. (2006) Oligomeric structure of the ATP-dependent protease La (Lon) of Escherichia coli, *Mol. Cells 21*, 129−134.
40. Dang, Q., and Frieden, C. (1997) New PC versions of the kinetic-simulation and fitting programs, KINSIM and FITSIM, *Trends Biochem. Sci. 22*, 317.
41. Frieden, C. (1994) Analysis of kinetic data: practical applications of computer simulation and fitting programs, *Methods Enzymol. 240*, 311−322.
42. Zimmerle, C. T., and Frieden, C. (1989) Analysis of progress curves by simulations generated by numerical integration, *Biochem. J. 258*, 381−387.

BI060809+